

# Enhanced tunability of the multiphoton absorption cross-section in seeded CdSe/CdS nanorod heterostructures

Xing, Guichuan; Chakraborty, Sabyasachi; Chou, Kok Loong; Nimai Mishra; Huan, Alfred  
Cheng Hon; Chan, Yinhai; Sum, Tze Chien

2010

Xing, G., Chakraborty, S., Chou, K. L., Nimai, M., Huan, A. C. H. Chan Y., Sum, T. C. (2010).  
Enhanced tunability of the multiphoton absorption cross-section in seeded CdSe/CdS  
nanorod heterostructures. Applied physics letters, 97.

<https://hdl.handle.net/10356/94162>

<https://doi.org/10.1063/1.3479048>

---

© 2010 American Institute of Physics. This paper was published in Applied Physics Letters  
and is made available as an electronic reprint (preprint) with permission of American  
Institute of Physics. The paper can be found at: [DOI: <http://dx.doi.org/10.1063/1.3479048>].  
One print or electronic copy may be made for personal use only. Systematic or multiple  
reproduction, distribution to multiple locations via electronic or other means, duplication  
of any material in this paper for a fee or for commercial purposes, or modification of the  
content of the paper is prohibited and is subject to penalties under law.

*Downloaded on 20 Mar 2024 17:34:16 SGT*

# Enhanced tunability of the multiphoton absorption cross-section in seeded CdSe/CdS nanorod heterostructures

Guichuan Xing,<sup>1</sup> Sabyasachi Chakraborty,<sup>2</sup> Kok Loong Chou,<sup>1</sup> Nimai Mishra,<sup>2</sup> Cheng Hon Alfred Huan,<sup>1</sup> Yinthai Chan,<sup>2</sup> and Tze Chien Sum<sup>1,a)</sup>

<sup>1</sup>*Division of Physics and Applied Physics, School of Physical and Mathematical Sciences, Nanyang Technological University, 21 Nanyang Link, Singapore 637371*

<sup>2</sup>*Department of Chemistry, National University of Singapore, 3 Science Drive 3, Singapore 117543*

(Received 22 March 2010; accepted 8 July 2010; published online 13 August 2010)

We present a method to separately tune the multiphoton absorption (MPA) and multiphoton excited photoluminescence using semiconductor core/enlarged-shell quantum dots (QDs), where the enlarged shell greatly enhances the MPA cross-sections while varying the core size facilitates emission wavelength selectivity. Following two-photon absorption (2PA) primarily in the shell and ultrafast charge-carrier localization to the core, luminescence occurs. We exemplify the validity of this method with CdSe/CdS nanorod heterostructures and find that the 2PA cross-section is enlarged to  $\sim 1.4 \times 10^6$  GM for 180 nm nanorods (with 800 nm, 150 fs laser pulse excitation) which is two to four orders larger than that of CdSe QDs. © 2010 American Institute of Physics.

[doi:10.1063/1.3479048]

Over the past two decades, multiphoton absorption (MPA) in colloidal semiconductor quantum dots (QDs) has been intensively investigated for potential applications in bioimaging, upconversion lasing, three-dimensional data storage and optical limiting.<sup>1–4</sup> These applications leverage on the following unique characteristics of QDs: size-dependent optoelectronic properties, large MPA cross-sections, relatively high quantum yields, good photostability, and flexible surface chemistry. Recently, the MPA cross-sections of QDs have been found to increase with size and this general trend has been attributed to a corresponding increase in the density of states.<sup>4–7</sup> Increasing the MPA cross-sections of QDs without significantly degrading its quantum yield or altering its emission wavelength can be highly desirable for example, in multiphoton fluorescence imaging where greater signal may be achieved using less average incident power, thus minimizing sample damage. While the pronounced size-dependence of the emission of fluorescent QDs in the strong confinement regime presents a convenient way to achieve desired emission wavelengths by simply changing the dot size, however, it also simultaneously imposes severe restrictions on the ability to vary the absorption cross-section while maintaining the emission at a required wavelength. Thus from the stand point of wavelength-specific applications, increasing the MPA cross-section of a QD without significantly modifying its size-dependent emission is an important and yet nontrivial challenge to overcome.

Herein we present a method that permits the independent tuning of the MPA cross-section and its corresponding luminescence properties using semiconductor core/enlarged-shell QDs. We demonstrate this with a representative CdSe/CdS nanodot/nanorod system. The elongated CdS shell is used as a photon-capturing “antenna,” which can greatly enhance the overall MPA cross-section of the QD. Photoexcitation of the CdS shell leads to ultrafast carrier transfer to the CdSe core where radiative recombination subsequently occurs.<sup>8</sup> We

show that further elongating the CdS shell in rods of a certain length result in substantial gains in the MPA cross-section without significantly redshifting their emission. The emission peak, on the other hand, can be tuned by appropriately changing the core size. Importantly, these results suggest a strategy for enhancing the MPA while independently tuning the emissive wavelengths of semiconductor QDs in a way which is highly relevant to their applications in multiphoton bioimaging and upconversion lasing.

The synthesis of the CdSe spherical core and the subsequent core/shell CdSe/CdS nanorod heterostructures with different aspect ratios were based on previously reported procedures with slight modifications (see Ref. 16).<sup>8</sup> The morphologies and size distributions of the as-prepared nanorod heterostructures were characterized with a transmission electron microscope (JEOL-JEM 2010F) operating at 200 kV. Representative TEM micrographs are shown in Fig. 1, which illustrate the uniformity and narrow size distribution of the various rods synthesized. The average rod diameter was estimated to be  $\sim 5$  nm for all four samples, while the average lengths were determined to be 8.5 nm, 34 nm, 39 nm, and

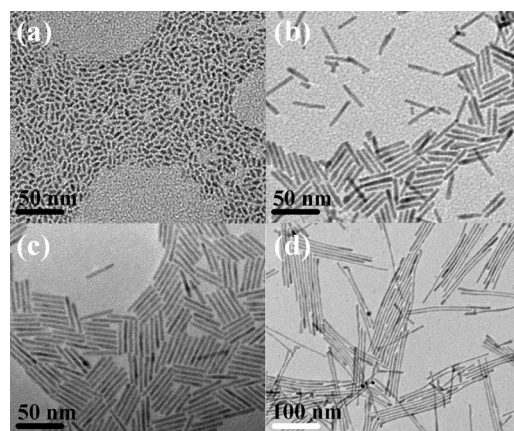


FIG. 1. TEM images of the CdSe/CdS nanodot/nanorod heterostructures with (a) 8.5 nm, (b) 34 nm, (c) 39 nm, and (d) 180 nm average length.

<sup>a)</sup>Electronic mail: tzechien@ntu.edu.sg.

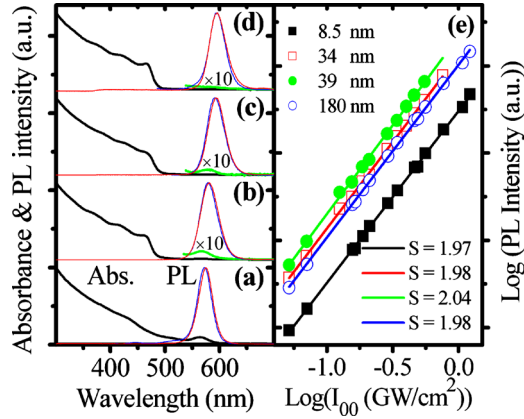


FIG. 2. (Color online) (a), (b), (c), and (d) show the normalized UV-visible absorption spectra (black) and its magnified ( $\times 10$ ) region (green [light gray]), as well as PL spectra corresponding to 400 nm (blue [dark gray]) and 800 nm (red [medium gray]) excitation of the 8.5 nm, 34 nm, 39 nm, and 180 nm long CdSe/CdS rods, respectively. (e) The corresponding log-log plots of the PL signals (normalized by particle number concentration) as a function of excitation power at 800 nm. The solid lines in (d) are the linear fittings.

180 nm, respectively. Histogram analysis yielded length dispersions that were less than 20%. The diameter of the CdSe core used was  $\sim 2.4$  nm, as estimated from its first absorption peak at 509 nm.<sup>5,9</sup> The quantum yields ( $\eta$ ) were determined to be 82%, 61%, 56%, and 8% for the 8.5 nm, 34 nm, 39 nm, and 180 nm CdSe/CdS nanorod heterostructures, respectively, and the declination of  $\eta$  with increasing rod length may be ascribed to reduced oscillator strength and a larger number of surface defects per nanorod.<sup>10</sup> Figures 2(a)–2(d) show the normalized room temperature linear absorption and one-photon excitation photoluminescence (PL) spectra of dilute concentrations of nanorod samples in toluene. The linear absorption profiles are dominated by the large CdS shell below 500 nm,<sup>8–11</sup> while the contribution from the CdSe core yields a peak at around 580 nm. Compared with the first absorption peak (at 509 nm) of the as-synthesized CdSe core, this value is significantly redshifted due to the delocalization of the electron into the shell, in agreement with previous reports.<sup>8–13</sup> A summary of the nanorod lengths,  $\eta$  and the respective positions of their peak PL is given in Table I.

One consequence of a type I (or quasitype II) core-shell energy profile is the electron is not delocalized across the entire length of the nanorod shell and the PL emission should not redshift beyond a certain rod length.<sup>8–13</sup> This is evident from our results in Table I where the PL emission peak shifts from 2.17 to 2.08 eV as the length is increased from 8.5 to 39 nm (for these samples that have the same CdSe core). The peak remains almost invariant when the rod length is increased subsequently to 180 nm. This redshift is insignificant compared to the case where the CdSe QDs are increased in size by  $\sim 1$  nm (e.g., from 2 to 3.1 nm results in a shift from

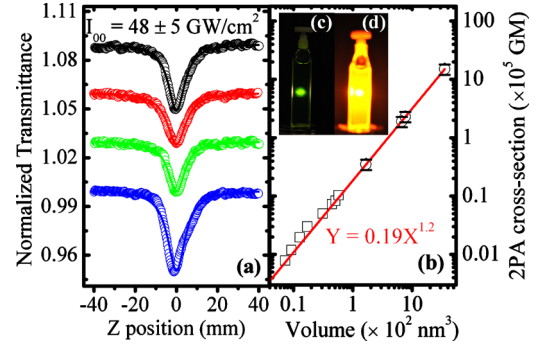


FIG. 3. (Color online) (a) Typical Open-aperture Z-scans at 800 nm for 8.5 nm (black), 34 nm (red [medium gray]), 39 nm (green [light gray]), and 180 nm (blue [dark gray]) CdSe/CdS nanodot/nanorod heterostructures, respectively. The solid lines are the fits with Eq. (1). (b) A plot of 2PA cross-section as a function of nanoparticle volume. The data for the spherical CdSe QDs ( $\square$ ) are taken from Ref. 5. The red line is a power-law fit. The insets show the image of R6G (c) and 39 nm CdSe/CdS heterostructures (d) of the same concentration under the same intensity 800 nm laser pulse excitation. Images were taken with the same camera exposure time.

2.39 to 2.21 eV).<sup>4</sup> Enlarging the CdSe core size to 3.5 nm in our heterostructures allows the PL to shift to 637 nm [see Ref. 16 (Fig. S4)]. These findings collectively highlight our proposed methodology for varying the emission wavelength in a strongly quantum confined nanostructure independently of its overall size.

To investigate the multiphoton excited PL properties of these heterostructures, a regenerative amplifier at 1 KHz delivering 800 nm laser pulses (150 fs pulse width) was used as the excitation source (see Ref. 16). The 800 nm excited up-conversion PL (UPL) spectra (red) are also shown in Figs. 2(a)–2(d) for the 8.5 nm, 34 nm, 39 nm, and 180 nm CdSe/CdS nanodot/nanorod samples, respectively, and are basically identical to the one-photon excitation PL spectra, as expected. Figure 2(e) depicts the nearly quadratic power dependence for their corresponding UPL signals, commensurate with a two-photon absorption (2PA) process, rather than an Auger recombination process.<sup>14</sup> In order to quantitatively determine the 2PA properties of these elongated shell nanostructures, we performed open aperture Z-scan experiments<sup>15</sup> (see Ref. 16) and the results are summarized in Fig. 3(a).

According to Z-scan theory for 2PA, the normalized transmittance may be described as<sup>15</sup>

$$T_{OA}(z) = \frac{1}{\pi^{1/2} q_0} \int_{-\infty}^{\infty} \ln[1 + q_0 \exp(-x^2)] dx, \quad (1)$$

where  $q_0 = \alpha_2 I_0 L_{\text{eff}}$ ,  $L_{\text{eff}} = [1 - \exp(-\alpha_0 L)] / \alpha_0$ , and  $\alpha_0$  and  $\alpha_2$  are the linear and 2PA absorption coefficients, respectively.  $I_0 = I_{00} / (1 + z^2 / z_0^2)$  is the incident intensity,  $I_{00}$  is the on axis peak power and  $z_0 = \pi \omega_0^2 / \lambda$  is the Rayleigh range. From the best fit of the data, the 2PA coefficients can be extracted as 0.011 cm/GW, 0.0087 cm/GW, 0.0087 cm/GW, and 0.014 cm/GW for the 8.5 nm, 34 nm, 39 nm, and 180 nm CdSe/

TABLE I. CdSe/CdS heterostructures' length, PL emission peak, quantum yield, and 2PA cross-section.

Average length (nm)	8.5	34	39	180
PL emission peak (eV)	2.17	2.14	2.09	2.08
Quantum yield (%)	82	61	56	8
TPA cross-section <sup>a</sup> $\sigma_2$ (cm <sup>4</sup> s photon <sup>-1</sup> )	$0.35 \times 10^{-45}$	$1.9 \times 10^{-45}$	$2.3 \times 10^{-45}$	$14 \times 10^{-45}$

<sup>a</sup>Experimental uncertainty:  $\pm 20\%$ . Size dispersion:  $\leq 20\%$ .

CdS heterostructures, respectively. Next, the 2PA cross-section ( $\sigma_2$ ) per nanorod was calculated as<sup>15</sup>

$$\sigma_2 = 5\alpha_2\hbar\omega/N, \quad (2)$$

where  $\hbar\omega$  is the photon energy,  $N$  is the particle number concentration (i.e.,  $N_{8.5\text{ nm}} = 3.9 \times 10^{16}/\text{mL}$ ;  $N_{34\text{ nm}} = 5.6 \times 10^{15}/\text{mL}$ ;  $N_{39\text{ nm}} = 4.6 \times 10^{15}/\text{mL}$ ; and  $N_{180\text{ nm}} = 1.2 \times 10^{14}/\text{mL}$ ). A value of 5 was used for the correction factor for linear polarized excitation pulses on randomly oriented nanorods.<sup>8,10,17</sup> The obtained  $\sigma_2$  for different elongated shell lengths are listed in Table I, which clearly indicates that the  $\sigma_2$  increases with CdS shell length. For the 180 nm CdSe/CdS heterostructures, the  $\sigma_2$  is two to four-orders of magnitude larger than that of spherical CdSe QDs (Ref. 4) emitting at similar wavelengths and four-orders of magnitude larger than that of Rhodamine 6G (R6G).<sup>18</sup> As exemplified in the insets of Fig. 3, the UPL of the 39 nm nanorod (with the largest 2PA action cross-section ( $\sigma_2\eta$ ) among the four samples) is much more intense compared to that of R6G (at the same concentration) in methanol under the same experimental conditions.

The dependence of the  $\sigma_2$  on nanostructure volume is shown in Fig. 3(b). From the fit, a power-law dependence of  $1.2 \pm 0.1$  to the volume of the rod ( $V_{\text{rod}}$ ) is obtained. As a comparison, a 2PA power-law dependence of 4 and  $3.5 \pm 0.5$  to the diameter of spherical CdSe QDs were previously reported by He *et al.*<sup>4</sup> and Pu *et al.*,<sup>5</sup> respectively, in close agreement with our result (given  $\sigma_{2\text{PA}} \propto R^{3.5} \approx V^{1.17}$ ). For volume normalized  $\sigma_2$ , the near linear dependence from the fit clearly shows that it increases with nanostructure volume. A similar trend can be obtained for spherical QDs. This indicates that the 2PA enhancement is mainly dependent on the volume of the nanostructure and independent of its shape. Nonetheless, our method affords one the means to enhance the MPA without significantly redshifting the emission. While some reports claimed that the  $\sigma_2$  of spherical semiconductor QDs increase with decreasing QD size at certain wavelengths due to an increase in the oscillator strength at those corresponding excitonic transitions,<sup>19,20</sup> other investigations proposed that the  $\sigma_2$  generally increase with QD size in accordance with an increased density of states.<sup>6,7</sup> While it is possible that the 2PA cross-section at certain excitation wavelengths exhibit higher values at shorter nanorod lengths,<sup>19–21</sup> our findings suggest that the 2PA cross-section at our chosen excitation wavelength generally increases as the size of the rodlike shell is elongated, consistent with a model of an increased density of states. In summary, we

report on a method that allows the MPA and the multiphoton excited luminescence to be independently tunable.

This work is supported by the following research grants: NTU start-up grant (Grant No. M58110068); Academic Research Fund (AcRF) Tier 1—RG 49/08 (Grant No. M52110082); Science and Engineering Research Council (SERC) grant (Grant No. 042 101 0014), Agency for Science, Technology, and Research (A\*STAR), Singapore; and a NUS start-up grant (Grant No. WBS-R143-000-367-133).

<sup>1</sup>D. R. Larson, W. R. Zipfel, R. M. Williams, S. W. Clark, M. P. Bruchez, F. W. Wise, and W. W. Webb, *Science* **300**, 1434 (2003).

<sup>2</sup>C. Zhang, F. Zhang, T. Zhu, A. Cheng, J. Xu, Q. Zhang, S. E. Mohny, R. H. Henderson, and Y. A. Wang, *Opt. Lett.* **33**, 2437 (2008).

<sup>3</sup>X. Li, C. Bullin, J. W. M. Chon, R. A. Evans, and M. Gu, *Appl. Phys. Lett.* **90**, 161116 (2007).

<sup>4</sup>G. S. He, K. T. Yong, Q. D. Zheng, Y. Sahoo, A. Baev, A. I. Rysanyanskiy, and P. N. Prasad, *Opt. Express* **15**, 12818 (2007).

<sup>5</sup>S. C. Pu, M. J. Yang, C. C. Hsu, C. W. Lai, C. C. Hsieh, S. H. Lin, Y. M. Cheng, and P. T. Chou, *Small* **2**, 1308 (2006).

<sup>6</sup>L. A. Padilha, J. Fu, D. J. Hagan, and E. W. Van Stryland, *Opt. Express* **13**, 6460 (2005).

<sup>7</sup>L. A. Padilha, J. Fu, D. J. Hagan, E. W. V. Stryland, C. L. Cesar, L. C. Barbosa, C. H. B. Cruz, D. Buso, and A. Martucci, *Phys. Rev. B* **75**, 075325 (2007).

<sup>8</sup>D. V. Talapin, R. Koeppel, S. Gotzinger, A. Kornowski, J. M. Lupton, A. L. Rogach, O. Benson, J. Feldmann, and H. Weller, *Nano Lett.* **3**, 1677 (2003).

<sup>9</sup>W. W. Yu, L. Qu, W. Guo, and X. Peng, *Chem. Mater.* **15**, 2854 (2003).

<sup>10</sup>L. Carbone, C. Nobile, M. D. Giorgi, F. D. Sala, G. Morello, P. Pompa, M. Hytch, E. Snoeck, A. Fiore, I. R. Franchini, M. Nadasan, A. F. Silvestre, L. Chiodo, S. Kudera, R. Cingolani, R. Krahne, and L. Manna, *Nano Lett.* **7**, 2942 (2007).

<sup>11</sup>J. Müller, J. M. Lupton, P. G. Lagoudakis, F. Schindler, R. Koeppel, A. L. Rogach, and J. Feldmann, *Nano Lett.* **5**, 2044 (2005).

<sup>12</sup>A. Sitt, F. D. Sala, G. Menagen, and U. Banin, *Nano Lett.* **9**, 3470 (2009).

<sup>13</sup>M. G. Lupo, F. D. Sala, L. Carbone, M. Zavelani-Rossi, A. Fiore, L. Luer, D. Polli, R. Cingolani, L. Manna, and G. Lanzani, *Nano Lett.* **8**, 4582 (2008).

<sup>14</sup>G. Xing, W. Ji, Y. Zheng, and J. Y. Ying, *Appl. Phys. Lett.* **93**, 241114 (2008).

<sup>15</sup>M. Sheik-Bahae, A. A. Said, T. H. Wei, D. J. Hagan, and E. W. V. Stryland, *IEEE J. Quantum Electron.* **26**, 760 (1990).

<sup>16</sup>See supplementary material at <http://dx.doi.org/10.1063/1.3479048> for the synthesis details, the PL spectrum, and the experimental details.

<sup>17</sup>M. A. Bopp, Y. Jia, G. Haran, E. A. Morlino, and R. M. Hochstrasser, *Appl. Phys. Lett.* **73**, 7 (1998).

<sup>18</sup>M. A. Albota, C. Xu, and W. W. Webb, *Appl. Opt.* **37**, 7352 (1998).

<sup>19</sup>A. P. Alivisatos, *Science* **271**, 933 (1996).

<sup>20</sup>A. D. Lad, P. P. Kiran, D. More, G. R. Kumar, and S. Mahamuni, *Appl. Phys. Lett.* **92**, 043126 (2008).

<sup>21</sup>D. V. Talapin, J. H. Nelson, E. V. Shevchenko, S. Aloni, B. Sadtler, and A. P. Alivisatos, *Nano Lett.* **7**, 2951 (2007).